Data in Brief 37 (2021) 107231

Contents lists available at ScienceDirect

Data in Brief

journal homepage: www.elsevier.com/locate/dib

Data Article

PET NEMA IQ Phantom dataset: image reconstruction settings for quantitative PET imaging

Habibeh Vosoughi[a,b], Mohsen Hajizadeh[a], Farshad Emami[b], Mehdi Momennezhad[c,*], Parham Geramifar[d,*]

[a] Department of Medical Physics, Mashhad University of Medical Science, Mashhad, Iran
[b] Nuclear Medicine and Molecular Imaging Department, Imam Reza International University, Razavi Hospital, Mashhad, Iran
[c] Nuclear Medicine Research Center, Faculty of Medicine, Mashhad University of Medical Sciences, Mashhad, Iran
[d] Research Center for Nuclear Medicine, Shariati Hospital, Tehran University of Medical Science, Tehran, Iran

ARTICLE INFO

Article history:
Received 17 February 2021
Revised 9 June 2021
Accepted 10 June 2021
Available online 18 June 2021

Keywords:
PET/CT
Image Reconstruction
Quantitative Analysis
Phantom Study

ABSTRACT

The data presented here provide information about the role of reconstruction parameters on Positron Emission Tomography (PET) image quantification. Multiple phantom measurements in four different Spheres to Background Ratio (SBR) were performed on Biograph 6 TruePoint TrueV PET/CT scanner. PET raw data were reconstructed with/without resolution recovery algorithm using six various iteration x subsets with five different Full-Width Half-Maximum (FWHM) values of Gaussian post-smoothing filter. The Recovery Coefficient (RC) of six spheres using three common Volume of Interest (VOI) methods (max, 3D-50% Isocontour, and peak) were calculated. Moreover, SUV_{max}, SUV_{mean}, and SUV_{peak} and volumetric indices, such as metabolic tumor volume (MTV), volume recovery coefficient (VRC), and total lesion glycolysis (TLG) were measured. RC_{max}, $RC_{50\%}$, and RC_{peak} as a function of sphere size were plotted in all reconstruction methods considering different SBRs. The data could be noticeable for standardization and optimization of quantitative metrics in PET imaging.

* Corresponding authors.
E-mail addresses: MomennezhadM@mums.ac.ir (M. Momennezhad), pgeramifar@tums.ac.ir (P. Geramifar).

https://doi.org/10.1016/j.dib.2021.107231

Specifications Table

Subject	Medical imaging, Nuclear medicine
Specific subject area	PET/CT imaging, Reconstruction setting, Phantom study
Type of data	Graphs
How data were acquired	Data were acquired using Biograph 6 TruePoint TrueV PET/CT scanner (Siemens Healthcare, Erlangen, Germany) and analyzed using Syngo® software, SIEMENS Medical Solution.
Data format	Raw and Analyzed
Parameters for data collection	The impact of reconstruction parameters on quantitative indices, such as RC_{max}, $RC_{50\%}$, RC_{peak}, SUV_{max}, SUV_{mean}, SUV_{peak}, MTV, VRC, and TLG was assessed regarding various SBRs and sphere sizes of NEMA IQ phantom. Also, CNR and background variability was obtained.
Description of data collection	NEMA IQ phantom data acquisition was performed in 10 minutes list mode in different SBR values (4:1, 6:1, 8:1, and 10:1). Raw data of PET images were reconstructed by iteration x subsets of 2 × 8, 2 × 14, 4 × 8, 2 × 21, 4 × 14, 3 × 21 with 2, 4, 6, 8, and 10 mm FWHM of Gaussian post-smoothing filter. Two different algorithms of 3D-OSEM and PSF correction were applied.
Data source location	Institution: Razavi Hospital City/Town/Region: Mashhad Country: Iran
Data accessibility	Repository name: Vosoughi, Habibeh; Geramifar, Parham (2021), "PET NEMA IQ phantom dataset for quantification study", Mendeley Data, V2, https://doi.org/10.17632/zbz4rcjywc.2 Direct URL to data: http://dx.doi.org/10.17632/zbz4rcjywc.2

Value of the Data

- These data can be immensely helpful as a template for medical physicists who are concerned with PET/CT quantification optimization.
- These data specify the impact of different reconstruction settings on quantitative parameters regarding lesion size and activity concentration to background ratio.
- The obtained data could be beneficial for comparison with quantitative data obtained from different scanners in order to help researchers reducing inter-scanner variability.

1. Data Description

PET imaging has the potential to produce quantitative images of tracer uptake and was developed as a quantitative tool using SUV index 1[,2]. Although SUV is widely available and convenient to use in clinical routine reporting, it is significantly influenced by reconstruction parameters and VOI definition [1,3]. Also, resolution recovery, as an advanced algorithm, dramatically affects the PET quantification [4].

Our data consisted of raw and analyzed data. The quantitative dataset includes four Excel spreadsheets for four various SBRs that are available on the Mendeley data. Six quantitative metrics, including RC_{max}, $RC_{50\%}$, RC_{peak}, SUV_{max}, SUV_{mean}, and SUV_{peak}, and three volumetric indices of MTV, VRC, and TLG in different reconstruction settings were represented in these Excel files. Also, the contrast to noise ratio (CNR) and background variability were evaluated as image quality parameters. All metrics were calculated in six different sphere sizes of NEMA IQ phantom.

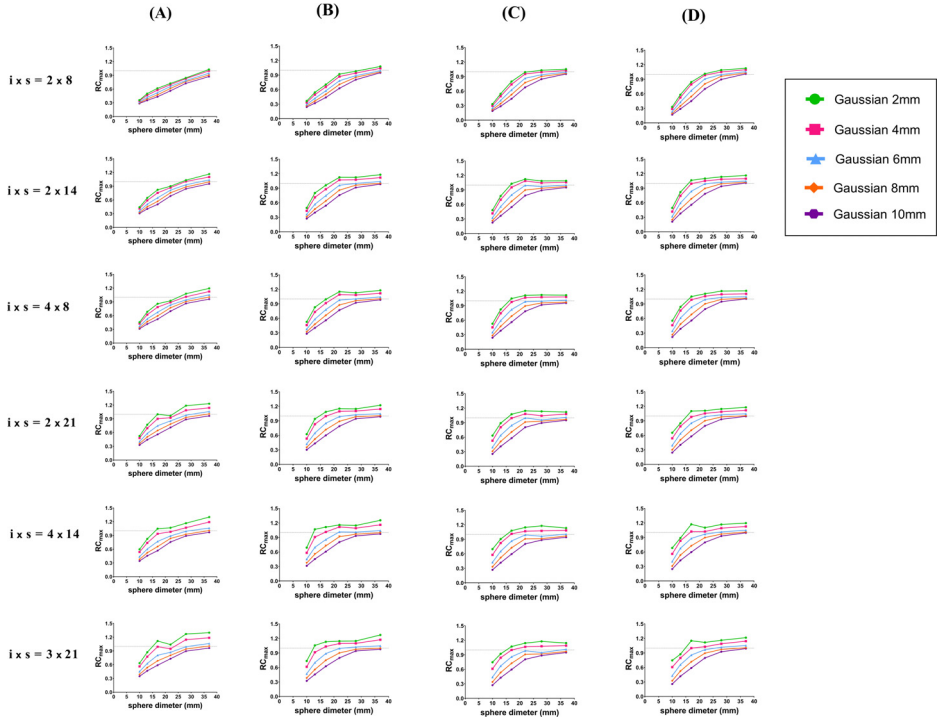

Fig. 1. RC_{max} vs. sphere diameters. These plots show the effect of 3D-OSEM image reconstruction algorithm using six iteration x subset (IXS) with various FWHM of Gaussian filter in different SBR. Each row represents constant IXS and columns represent; (A) SBR 4:1, (B) SBR 6:1, (C) SBR 8:1 and (D) SBR 10:1. In each plot impact of 2, 4, 6, 8 and 10 mm FWHM in constant IXS was shown. Dot line shows ideal RC value equal to 1.

As RC is a standard and useful indicator of scanner performance and the effect of reconstruction methods on quantification [5], RCs against sphere sizes in various reconstruction settings (different combinations of sub-iterations with various FWHM of Gaussian filters using 3D-OSEM with or without PSF correction algorithm) were assessed in this study. Reconstruction parameters were assessed in three commonly VOIs, four SBRs, and six sphere sizes of NEMA IQ phantom. Using the 3D-OSEM algorithm, RC_{max}, $RC_{50\%}$, and RC_{peak} against the diameter of spheres were plotted in Figs. 1, 2 and 3, respectively. Also, RC_{max}, $RC_{50\%}$, and RC_{peak} against sphere diameter using resolution modelling were illustrated in Figs. 4–6, respectively.

Volumetric indices were measured from only PET images. CNR for the smallest sphere with 10 mm diameter was evaluated to lesion detection in SBR4:1. In both algorithms with low level of smoothing CNR was less than 5, therefore according to ROSE criteria, this sphere was not observed in PET images and measurement of volumetric index was not possible. It was shown by zero in the published Excel files in the Mendeley data.

2. Experimental Design, Materials and Methods

2.1. Phantom preparation

Standard NEMA image quality phantom was used to collect data. This phantom contains a body compartment that is at least 18 cm in interior length, six fillable spheres with internal diameters of 10, 13, 17, 22, 28, and 37 mm with a wall thickness of not more than 1 mm, and a cylindrical insert with 5 cm outside diameter that is filled with low atomic number material

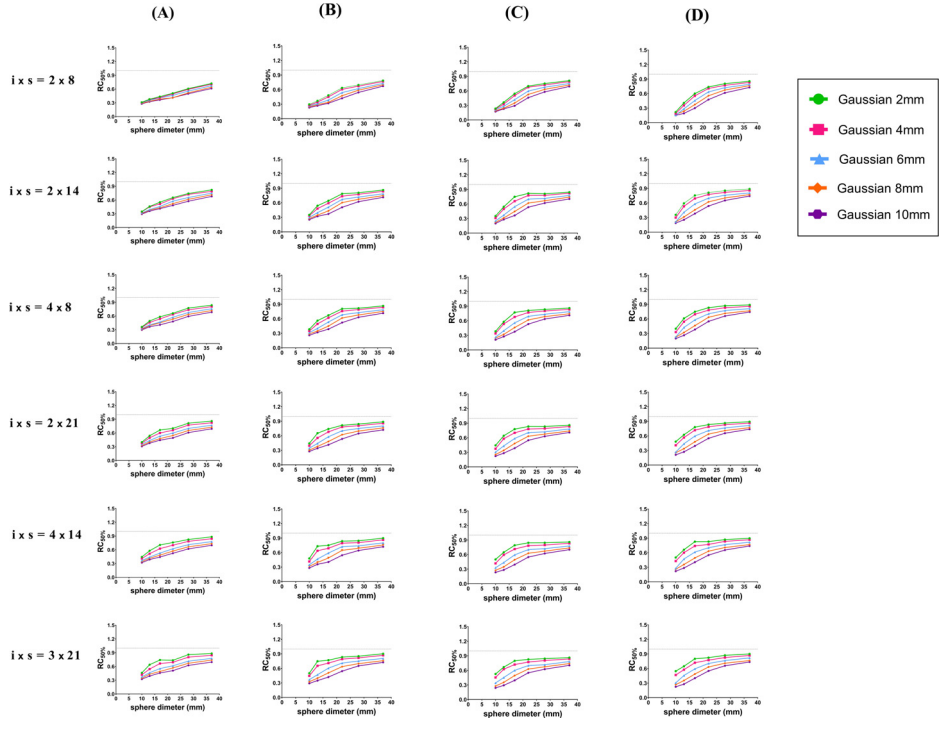

Fig. 2. $RC_{50\%}$ vs. sphere diameters. These plots show the effect of 3D-OSEM image reconstruction algorithm using six iteration x subset (IXS) with various FWHM of Gaussian filter in different SBR. Each row represents constant IXS and columns represent; (A) SBR 4:1, (B) SBR 6:1, (C) SBR 8:1 and (D) SBR 10:1. In each plot impact of 2, 4, 6, 8 and 10 mm FWHM in constant ixs was shown. Dot line shows ideal RC value equal to 1.

that mimics lung attenuation and is centred inside the body compartment and extends axially through the entire phantom.

The background of the phantom was filled with about 3.5 KBq/ml of the homogenous solution of ^{18}F-FDG. All spheres are filled with an ^{18}F-FDG solution at an activity concentration with either 4, 6, 8, and 10 times higher radioactivity concentration than the background to obtain SBR 4:1, 6:1, 8:1, and 10:1 (Fig. 7). Then, the spheres should be positioned in such a manner that the centers of all spheres should be in the same transverse slice.

2.2. Data acquisition

Data acquisition of the phantom was performed using the Biograph 6 TrueV PET/CT scanner (SIEMENS Healthcare, Erlangen, Germany) with a 6-slice spiral CT component. The technical specification of the scanner is 4.5 nsec coincidence window with 435–650 keV energy window. Data were collected using the time-based method in list mode format for 10 min. Several papers demonstrated that 3 min is suitable regardless of the brand and model of the PET/CT scanner [6,7]. However, evaluation of image quality on an this scanner demonstrated that the acquisition time could be adjusted to less than 3 min with respect to the patient's body weight of less than 60 kg and injected activity of 3.7 MBq/kg [8]. Therefore, 3 min duration per bed position was determined to mimic a clinical whole-body scan. According to the scanner performance specification, in the selected acquisition time, enough data were collected. Low-dose CT scans were obtained before PET scans for lesion localization, attenuation, and scatter corrections.

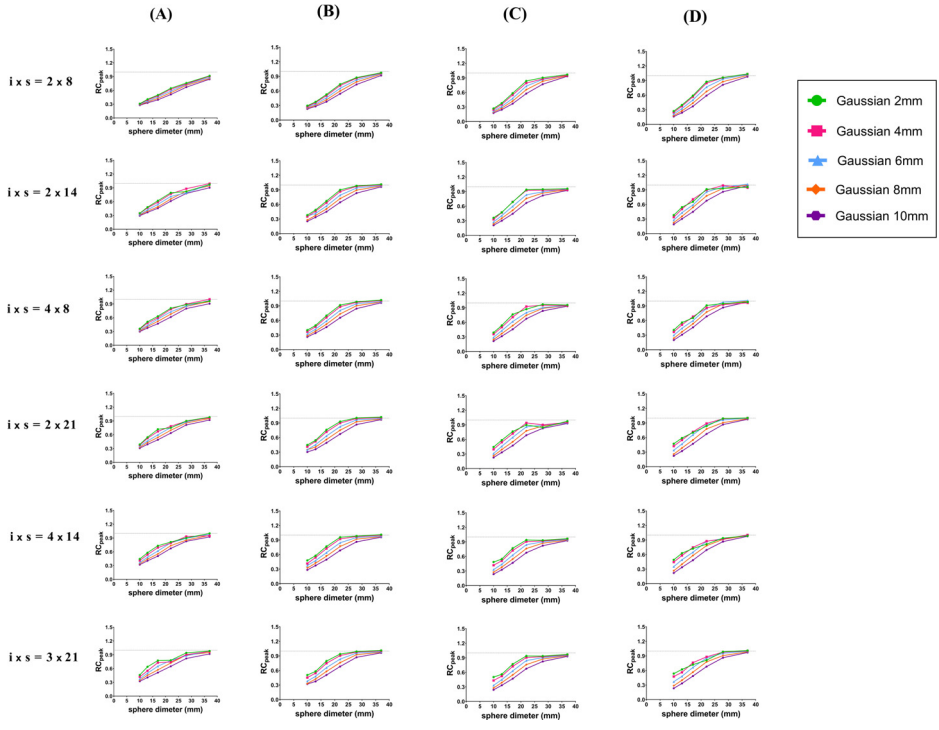

Fig. 3. RC_{peak} vs. sphere diameters. These plots show the effect of 3D-OSEM image reconstruction algorithm using six iteration x subset (IXS) with various FWHM of Gaussian filter in different SBR. Each row represents constant IXS and columns represent; (A) SBR 4:1, (B) SBR 6:1, (C) SBR 8:1 and (D) SBR 10:1. In each plot impact of 2, 4, 6, 8 and 10 mm FWHM in constant IXS was shown. Dot line shows ideal RC value equal to 1.

In this study we aimed to assess the effect of different reconstruction parameters on PET quantification and image quality. This assessment resulted in 240 reconstructed PET images with more than 1400 region of interest (ROI) based lesion (sphere) analysis. As we did not intend to provide absolute values but providing a framework to investigate the effect of the reconstruction parameter on the acquired data, we relied on QC procedures as a key aspect in the operation of PET/CT instrument and in the reliability of the data obtained. Thus, routine quality control tests were performed before phantom data acquisition. Moreover, the phantom preparation, data acquisition protocol and image analysis method was constant in each SBR. We also checked repeatability using cross calibration cylindrical phantom. We repeated cross calibration test in 3 different days and obtained the same results for Cross Calibration Correction Factor (CCCF).

2.3. Image reconstruction

Reconstruction was carried out using the available PET/CT scanner software. Axial compression is used in scanners or image reconstruction algorithms to reduce the size of data and computation times during reconstruction [9]. Axial compression of raw data in this scanner is based on span-11 resulted in 559 3D sinograms with 2 mm size. Raw PET data were reconstructed applying OSEM-3D image reconstruction algorithm or PSF modeling that are defined as TrueX in Syngo® software, SIEMENS Medical Solution. Images were reconstructed in six different iteration x subsets (I X S) with five FWHM values of Gaussian post-smoothing filters. Reconstruction settings are defined as:

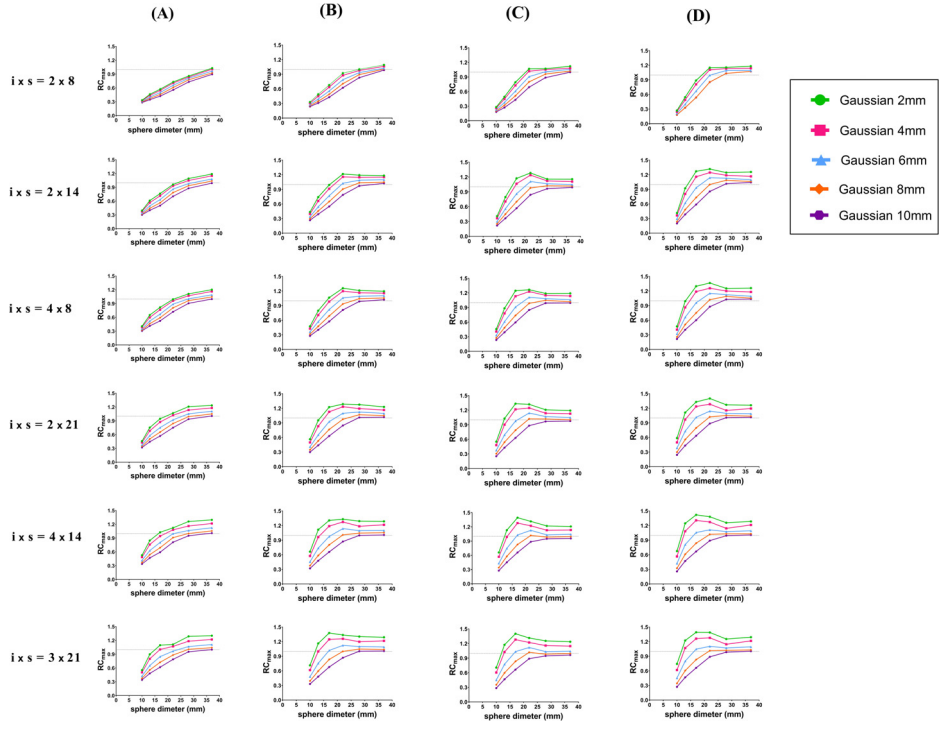

Fig. 4. RC_{max} vs. sphere diameters. These plots show the effect of 3D-OSEM+PSF reconstruction algorithm using six iteration x subset (IXS) with various FWHM of Gaussian filter in different SBR. Each row represents constant IXS and columns represent; (A) SBR 4:1, (B) SBR 6:1, (C) SBR 8:1 and (D) SBR 10:1. In each plot impact of 2, 4, 6, 8 and 10 mm FWHM in constant IXS was shown. Dot line shows ideal RC value equal to 1.

- I X S = 2 × 8 with 2, 4, 6, 8 and 10 mm FWHM
- I X S = 2 × 14 with 2, 4, 6, 8 and 10 mm FWHM
- I X S = 4 × 8 with 2, 4, 6, 8 and 10 mm FWHM
- I X S = 2 × 21 with 2, 4, 6, 8 and 10 mm FWHM
- I X S = 4 × 14 with 2, 4, 6, 8 and 10 mm FWHM
- I X S = 3 × 21 with 2, 4, 6, 8 and 10 mm FWHM

Totally, 60 combinations of i x s with Gaussian smoothing filter in two different algorithms were obtained for each SBR. Reconstructed matrix size was 168 × 168 resulting in a 4.07 × 4.07 × 2.027 mm voxel size. Normalization, Attenuation, Scatter, and Decay corrections were performed for all reconstructions to improve overall image quality. Scatter correction is an important component of image quality. In Biograph True point PET/CT scanners, scatter correction is performed applying model-based compton scatter correction using Monte Carlo-based computational technique. This single scatter simulation algorithm employs a unique, intuitive sampling technique organized as a summation over sample scattering points [10].

2.4. Data analysis

Quantitative analysis was performed using Recovery Coefficient (RC) that is defined as the ratio of measured to true activity concentration. The three most common and recommended Volume of Interest (VOI) definitions were applied to calculate RC in the spheres. The VOI methods were defined as the maximum voxel in the VOI (RC_{max}), 3D-50% mean of voxels (RC_{mean}),

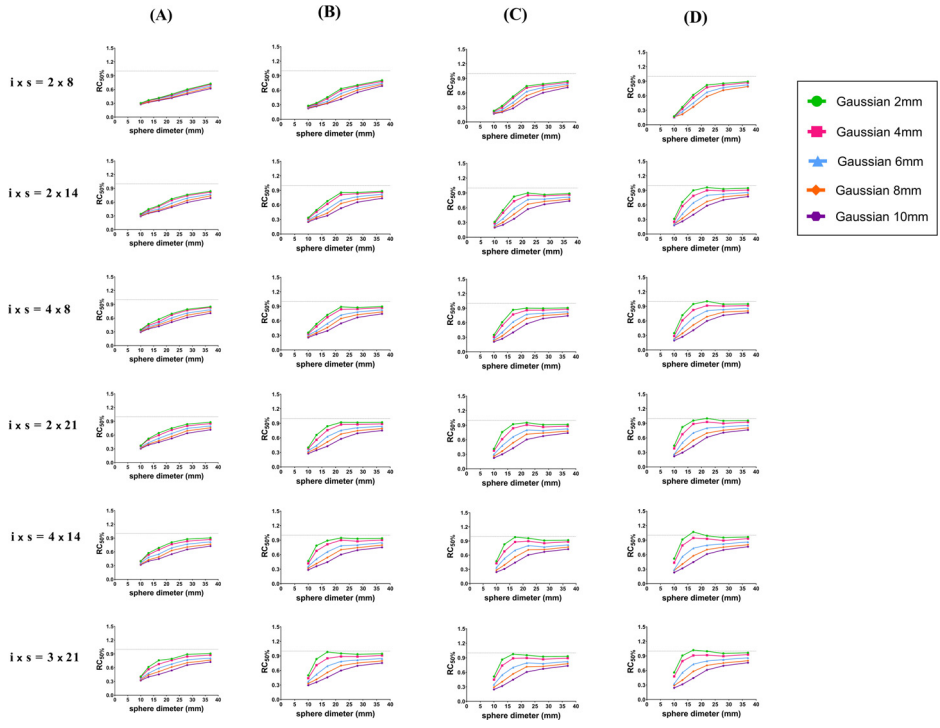

Fig. 5. $RC_{50\%}$ vs. sphere diameters. These plots show the effect of 3D-OSEM+PSF reconstruction algorithm using six iteration x subset (IXS) with various FWHM of Gaussian filter in different SBR. Each row represents constant IXS and columns represent; (A) SBR 4:1, (B) SBR 6:1, (C) SBR 8:1 and (D) SBR 10:1. In each plot impact of 2, 4, 6, 8 and 10 mm FWHM in constant IXS was shown. Dot line shows ideal RC value equal to 1.

and the mean voxels of spherical VOI with a volume of 1 cm^3 are placed in the highest uptake region (RC_{peak}). SUV in three different VOI definitions is calculated as follows:

$$SUV = \frac{\text{Activity concentration in region of interest (kBq/ml)}}{\text{total activity(kBq) / weight (kg)}}$$

MTV was defined for the voxels within the VOI with 50% of SUV_{max}. VRC was measured as the ratio of MTV and true sphere volume for the assessment of volumetric accuracy and TLG was calculated as a product of MTV and SUV_{mean} (TLG=MTV x SUV_{mean}).

For analysis, one transverse slice of the reconstructed image centered on spheres was selected such that all spheres are visualized with the highest contrast. The same slice should be used for the analysis of all spheres. Circular VOI was drawn on spheres with a diameter as close as possible to sphere diameters. Fig. 8 shows a sample indicating data analysis.

Maximum count in each VOI of spheres, the average count of 50% of max voxels, and average counts using peak definition were recorded as measured values. The ratio of the measured to true activity concentrations was determined for all spheres and VOI definitions as the RC value. In the end, the influence of reconstruction parameters was assessed for all RCs against sphere sizes in different activity concentrations to the background.

The effect of reconstruction settings on image quality was evaluated by CNR and background variability. Values of both parameters were represented in the Excel files. Background variability was calculated as the ratio of standard deviation and the average value of counts in the VOI of

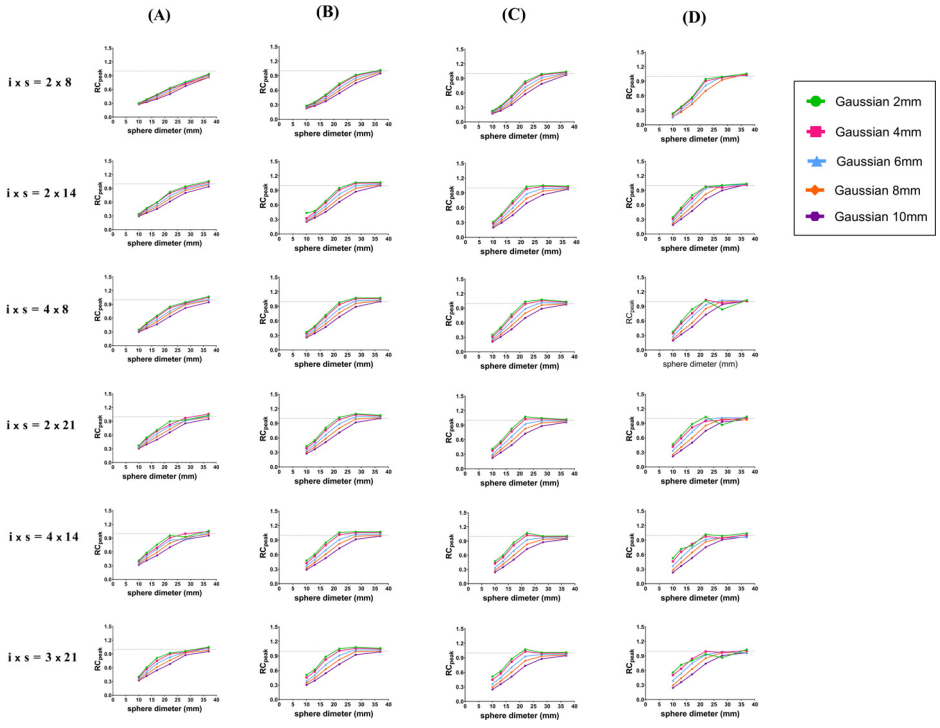

Fig. 6. RC_{peak} vs. sphere diameters. These plots show the effect of 3D-OSEM+PSF reconstruction algorithm using six iteration x subset (IXS) with various FWHM of Gaussian filter in different SBR. Each row represents constant IXS and columns represent; (A) SBR 4:1, (B) SBR 6:1, (C) SBR 8:1 and (D) SBR 10:1. In each plot impact of 2, 4, 6, 8 and 10 mm FWHM in constant IXS was shown. Dot line shows ideal RC value equal to 1.

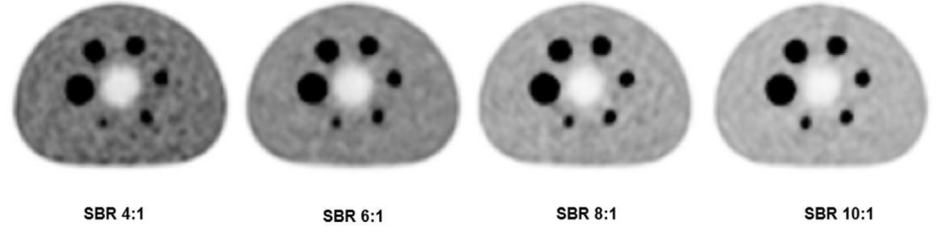

Fig. 7. Trans-axial slice of NEMA IQ phantom in four different SBR.

the phantom background. CNR was calculated using the below equation:

$$CNR = \frac{Cmean(sphere) - Cmean(background)}{SD\ (background)}$$

Twelve spherical diameters VOIs for each sphere size were drawn throughout the background and the average values of activity concentration for VOI was recorded as the C_{mean} background.

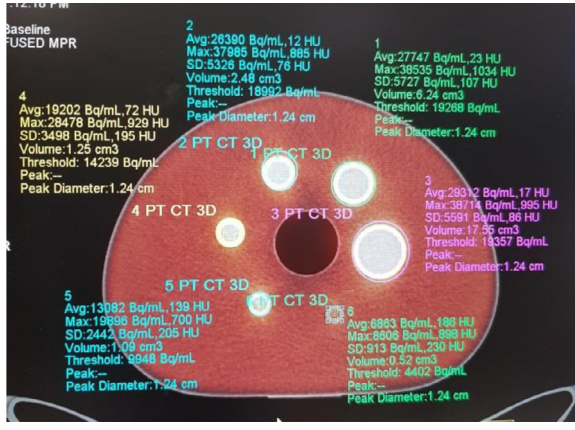

Fig. 8. A sample of data analysis in Syngo software.

Ethics Statement

This study was a phantom experiment and did not require ethics committee approval.

CRediT Author Statement

Habibeh Vosoughi: Methodology, Investigation, Writing- Original draft preparation; **Mohsen Hajizadeh:** Investigation, Funding acquisition, Supervision; **Farshad Emami**: Methodology, Investigation; **Mehdi Momennezhad:** Investigation, Visualization; **Parham Geramifar:** Methodology, Supervision, Writing and Editing, Project Administration.

Declaration of Competing Interest

None.

Acknowledgments

This data was collected as part of PhD thesis supported by Mashhad University of Medical Sciences (No. 961625) and cooperation of Nuclear Medicine Department of Razavi Hospital.

References

[1] R. Boellaard, Standards for PET image acquisition and quantitative data analysis, J. Nucl. Med. 50 (Suppl 1) (2009) 11S–20S.
[2] P.E. Kinahan, R.K. Doot, M. Wanner-Roybal, L.M. Bidaut, S.G. Armato III, Meyer C.R., et al., PET/CT assessment of response to therapy: tumor change measurement, truth data, and error, Transl. Oncol. 2 (4) (2009) 223.
[3] M.C. Adams, T.G. Turkington, J.M. Wilson, T.Z. Wong, A systematic review of the factors affecting accuracy of SUV measurements, Am. J. Roentgenol. 195 (2) (2010) 310–320.
[4] E. Prieto, I. Domínguez-Prado, M.J. García-Velloso, I. Peñuelas, J.Á. Richter, J.M. Martí-Climent, Impact of time-of-flight and point-spread-function in SUV quantification for oncological PET, Clin. Nucl. Med. 38 (2) (2013) 103–109.
[5] M.D. Kelly, J.M. Declerck, SUVref: reducing reconstruction-dependent variation in PET SUV, EJNMMI Res. 1 (1) (2011) 16.

[6] A. Sher, F. Lacoeuille, P. Fosse, L. Vervueren, A. Cahouet-Vannier, D. Dabli, et al., For avid glucose tumors, the SUV peak is the most reliable parameter for [18 F] FDG-PET/CT quantification, regardless of acquisition time, EJNMMI Res. 6 (1) (2016) 21.
[7] C. Brown, M.-F. Dempsey, G. Gillen, A.T. Elliott, Investigation of 18F-FDG 3D mode PET image quality versus acquisition time, Nucl. Med. Commun. 31 (3) (2010) 254–259.
[8] V.O. Menezes, M.A. Machado, C.C. Queiroz, S.O. Souza, F. d'Errico, M. Namías, et al., Optimization of oncological 18F-FDG PET/CT imaging based on a multiparameter analysis, Med. Phys. 43 (2) (2016) 930–938.
[9] M.A. Belzunce, A.J. Reader, Assessment of the impact of modeling axial compression on PET image reconstruction, Med. Phys. 44 (10) (2017) 5172–5186.
[10] C.C. Watson, M. Casey, C. Michel, B. Bendriem, editors. Advances in scatter correction for 3D PET/CT. IEEE Symposium Conference Record Nuclear Science 2004; 2004: IEEE.